Nuclear Engineering and Technology 55 (2023) 169–179

Contents lists available at ScienceDirect

Nuclear Engineering and Technology

journal homepage: www.elsevier.com/locate/net

Original Article

Study of hydrodynamics and iodine removal by self-priming venturi scrubber

Jawaria Ahad [a, *], Talha Rizwan [a], Amjad Farooq [a], Khalid Waheed [a], Masroor Ahmad [a], Kamran Rasheed Qureshi [b], Waseem Siddique [b], Naseem Irfan [a]

[a] *Department of Nuclear Engineering, Pakistan Institute of Engineering and Applied Sciences, Pakistan*
[b] *Department of Mechanical Engineering, Pakistan Institute of Engineering and Applied Sciences, Pakistan*

ARTICLE INFO

Article history:
Received 1 October 2021
Received in revised form
27 July 2022
Accepted 4 September 2022
Available online 9 September 2022

Keywords:
Filtered containment venting system
Nuclear powerplants
Severe accident mitigation
Venturi scrubber
Iodine removal
Environment safety
Mass transfer
Hazardous gas removal

ABSTRACT

Filtered containment system is a passive safety system that controls the over-pressurization of containment in case of a design-based accidents by venting high pressure gaseous mixture, consisting of air, steam and radioactive particulate and gases like iodine, via a scrubbing system. An indigenous lab scale facility was developed for research on iodine removal by venturi scrubber by simulating the accidental scenario. A mixture of 0.2 % sodium thiosulphate and 0.5 % sodium hydroxide, was used in scrubbing column. A modified mathematical model was presented for iodine removal in venturi scrubber. Improvement in model was made by addition of important parameters like jet penetration length, bubble rise velocity and gas holdup which were not considered previously. Experiments were performed by varying hydrodynamic parameters like liquid level height and gas flow rates to see their effect on removal efficiency of iodine. Gas holdup was also measured for various liquid level heights and gas flowrates. Removal efficiency increased with increase in liquid level height and gas flowrate up to an optimum point beyond that efficiency was decreased. Experimental results of removal efficiency were compared with the predicted results, and they were found to be in good agreement. Maximum removal efficiency of 99.8% was obtained.

1. Introduction

Nuclear powerplants are reliable and clean source of energy. They are designed articulately with wide safety margins and various safety systems, fully capable to handle design-based accidents. However, accidents like Three- Mile Island, Chernobyl and Fukushima showed the world that beyond design-based accidents can compromise the integrity of containment. Containment is the last physical barrier which refrains the radioactive gases to spread into environment. Severe accidents often result in production of steam and the resulting rise of pressure beyond designed limit can lead to explosion or ruptures causing spread of radioactivity into environment. Release of hazardous fission products like elemental and organic iodine and cesium iodide as a result of core meltdown are normally associated with these kinds of accidents. These gases if spread into environment can cause thyroid cancer. After Fukushima, a lot of research was done on accident mitigation and safety systems. As a result of this research, a system named Filtered Containment Venting system was recommended as a solution to this problem [1].

Filtered Containment Venting System (FCVS) is a passive system that limits excessive pressure buildup in containment, maintains structural integrity of the containment, provides retention of radiotoxicity and vents the clean air into atmosphere. In case of a severe accident, when containment pressure rises above set limit, some part of steam along with mixture of gases is released from containment to this system via isolation valves to maintain over-pressurization. After this, the incoming mixture of gases are filtered in a scrubbing tank, and clean air is vented out into the environment. FCVS has become a vital safety requirement after Fukushima accident and most of the countries have already made it a part of their new powerplants and others are considering it [2]. Few of the requirements for FCVS include decontamination factor of >100 for iodine i.e. >99% removal efficiency, capability of removing a few grams to tens of grams of iodine and to work at its full capacity for 24 h [3].

* Corresponding author.
E-mail address: jawariahad@gmail.com (J. Ahad).

https://doi.org/10.1016/j.net.2022.09.005

Different scrubbers have been used in FCVS for removal of radioactive Iodine. Among them, venturi scrubbers are the most widely used scrubbers. Venturi scrubbers have been used for various applications of pollution control since its discovery by Giovanni Battista Venturi in 1797 [4]. In 1954, use of venturi scrubber for gas and aerosol removal was initiated [5] and it has been in use ever since [6]. Operational parameters of venturi scrubber play a vital role in the development of FCVS. A lot of research has been done in the past to study hydrodynamic characteristics of venturi scrubber by using mathematical and experimental approach. Several mathematical models have been presented to calculate hydrodynamic characteristics of venturi such as droplet size, pressure drop, bubble dynamics and mass transfer etc. Nukiyama presented a correlation for calculation of droplet diameter in venturi scrubber, but it was for a specific range of throat velocities [7]. Later, a more versatile correlation for calculation of droplet diameter was presented by Boll et al., for a very vast range of throat velocities [8].

Gas holdup is another very important parameter to study the hydrodynamic behavior of venturi scrubber. A lot of research has been done in this area for bubble reactors and columns but not so much for venturi scrubbers. It is a dimensionless parameter that depicts the fraction of gas present in gas bubbles. Hughmark presented a correlation for gas holdup by taking into account properties of liquid and the predicted values were in agreement with experimental results with 11% standard deviation [9]. Hikita and Kikukawa studied effect of different liquids on gas holdup for bubble columns with different diameters. A correlation was also presented to predict gas hold up with deviation of 1.4–3.6% [10]. Kumar et al., proposed a new correlation for gas holdup by incorporating superficial gas velocity, density of liquid and gas and surface tension. Superficial gas velocity was observed to have a significant effect on holdup [11]. Sal et al., proposed a correlation for gas hold up based on dimensions of orifice and column and dimensionless numbers [12]. Sasaki et al., also presented a new empirical correlation for gas holdup by taking into account geometrical dimensions, Froude number based on initial height of liquid and superficial gas velocity. Gas holdup was observed to be decreasing with increase of liquid height [13]. Table 1 summarizes various correlation developed for gas holdup.

Mass transfer is the limiting factor in removal of unwanted component from gas streams. Most of the mass transfer occurs via droplets and film at the throat of venturi and via bubbles in column, where liquid and gas interact with each other. Gamisan et al., proposed a model for mass transfer in venturi scrubber. The breakup of liquid into droplets and film was studied. The basic equation was derived from Azzopardi's work by solving boundary layer equations for momentum and mass balance in two-phase flow and cylindrical coordinates for two phase flow [14]. Model was implemented on Industrial scale ejector venturi scrubber. Reaction was considered to be instantaneous due to short contact time of venturi scrubbers. And droplet size was considered to be spherical. Results indicated a significant increase in mass transfer rate due to liquid film. Removal efficiency was observed to be increased with increase in liquid film thickness. Theoretical results were in good agreement with mathematical results [15].

A lot of experimental research has been done to study the effect of different operational parameters on removal efficiency of venturi scrubber. Ali et al., measured removal efficiency of iodine for submerged and non-submerged venturi scrubber. He studied the effect of various parameters including gas flow rate, liquid flow rate, concentration of iodine etc. on removal efficiency. Iodine removal efficiency was calculated to be 0.099 ± 0.001. Comparison of calculated and experimental values showed good agreement for submerged case but calculations underpredicted the results for non-submerged venturi [16,17]. Gulhane measured removal efficiency of iodine and pressure drop in venturi scrubber. Removal efficiency came out to be 41–66 %. Low removal efficiency was due to deposition of iodine on the surface, less accurate measurement techniques and low solubility of iodine in water [18]. Bal studied removal efficiency of iodine by using water and potassium iodide as scrubbing solution. Maximum removal efficiency obtained from water was 70.13% and maximum removal efficiency obtained from KI was 82.32 % [19]. Jung performed experiment for removal efficiency of iodine and methyl iodide in the large-scale ARIEL facility of Korea. Decontamination factor of over 1000 was obtained for iodine and over 500 for methyl iodide [20]. Zhou studied removal efficiency of iodine vapors by varying different operational parameters like temperature, gas and liquid flow rates. Removal efficiency obtained was about 99%. A mathematical model was also proposed for the calculation of removal efficiency and results were comparable to experimental results [21].

Table 1
Gas holdup correlations.

Sr. No	Correlation	Author
1	$\varepsilon_g = \dfrac{1}{2+\left(\dfrac{0.35}{v_{sg}}\right)\left[\left(\dfrac{\rho_l}{1}\right)\left(\dfrac{\sigma}{72}\right)\right]^{1/3}}$	Hughmark [9].
2	$\varepsilon_g = 0.505 v_{sg}^{0.47}\left(\dfrac{72}{\sigma}\right)^{\frac{2}{3}}\left(\dfrac{1}{\mu_l}\right)^{0.05}$	Hikita and Kikukawa [10].
3	$\varepsilon_g = 0.728U - 0.485U^2 + 0.0975U^3$ $U = v_{sg}\left(\dfrac{\rho_l^2}{\sigma \Delta\rho g}\right)^{1/4}$	Kumar et al. [11],
4	$\varepsilon_g = 0.672 g^{-0.131} v_{sg}^{0.578} \rho_g^{0.062} \rho_l^{0.069} \mu_g^{0.107} \mu_l^{-0.053} \sigma^{-0.185}$	Hikita et al. [14],
5	$\varepsilon_g = 0.2278\left[\dfrac{Fr^{0.7767} Ar^{0.3649}\left(\dfrac{d_o}{d_c}\right)^{0.4780}}{E_o^{0.3916} We^{0.2402}}\right]$ $Ar = \dfrac{d_o^3 \rho_l^2 g}{\mu_l^2}, E_o = \dfrac{d_o^2 \rho_l^2 g}{\sigma_l}, W_e = \dfrac{d_c^4 v_{sg}^2 \rho_l}{d_o^3 N^2 \sigma_L}, Fr = \dfrac{v_{sg}^2}{d_o g}$	Sal et al. [12],
6	$\varepsilon_g = \dfrac{C_1 Fr_H}{1 + C_2 Fr_H}$ where $Fr_H = \dfrac{v_{sg}}{\sqrt{g H_o}}$, $C_1 = 19.2$ & $C_2 = 56.4$	Sasaki et al. [13],

Iodine removal is very important to ensure safety of people and environment. In order to get maximum iodine removal efficiency, hydrodynamic behavior of venturi scrubber must be studied in detail [22]. A modified and improved mathematical model was presented for estimation of removal efficiency in venturi and column. Improvement was made by incorporating very important parameters like jet penetration length in venturi, bubble rise velocity and gas holdup in the column which were not considered before. These parameters play a huge role in correct estimation of liquid-gas contact time and hence removal efficiency and their inclusion are necessary to predict removal efficiency of iodine. A lab scale experimental setup was developed indigenously to study the factors affecting removal efficiency of iodine. Effect of gas flowrate and liquid level height were studied in this research as they are the most important parameters that controls the removal efficiency. Previous research just explained the general trend but, in this research, optimized values of gas flowrate and liquid level height were measured. Gas holdup is also a very important operating parameter but the research regarding this parameter in venturi scrubber is scarce to the best of author's knowledge. So, gas holdup was also measured in venturi scrubber for various gas flowrates and liquid level heights. Different correlations of gas holdup were compared with experimental results to find the best match. Comparison of experimental and predicted results for removal efficiency was also made.

2. Mathematical model

A mathematical model is developed to estimate the mass transfer in venturi as well as in the bubble column. Fig. 1 a) shows the concentration of contaminated air stream passing through the system. For the calculation in venturi, where water is in dispersed phase, the mass transfer occurs at the droplet surface. The initial concentration of contaminated air is taken as C_{in} and the air leaving the venturi has a concentration C_{out} . The same air when enters the bubble column, where air is in disperse phase, the mass transfer occurs at the bubble surface. The inlet contaminant concentration in the bubble column is taken same as exit concentration at venturi (C_{out}) denoted in this case by C'_{in} , and the bubble column exit concentration is denoted as C'_{out} . The final removal efficiency is calculated as the cumulative removal of contaminant in venturi and bubble column. The gas holdup is also measured experimentally by measurement of increase in water level due to gas. Abbreviations for sections of venturi, used in the model are shown in Fig. 1 b).

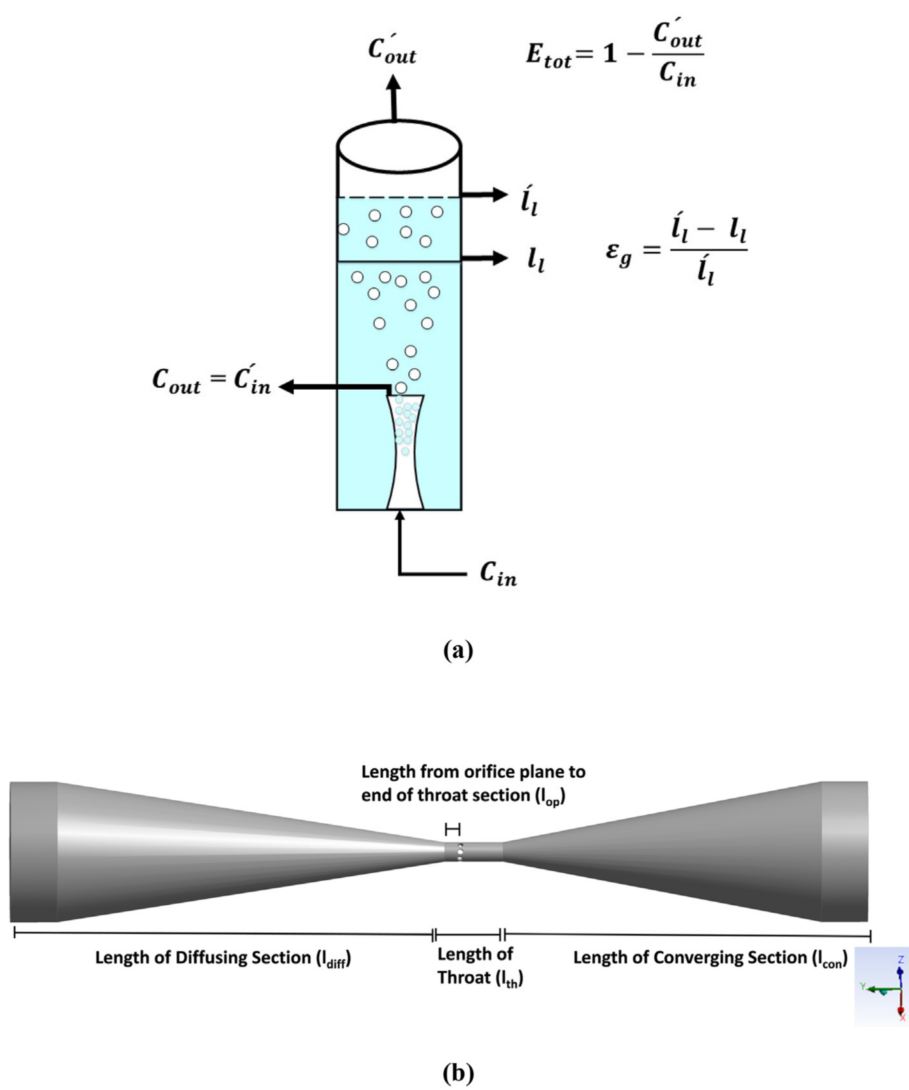

Fig. 1. (a) Submerged venturi scrubber (b) sections of venturi.

2.1. Mass transfer model for removal efficiency in venturi

Mass transfer model for venturi is based on two film theory of mass transfer proposed by Gamisan et al. [15],and it was used by Ali et al. [17], for iodine removal in venturi scrubber. Driving force is concentration difference of iodine and mass transfer occurs at the interface of air and liquid films. Current model is a modified version of model presented by Ali et al., [17]. For venturi, mass transfer took place by droplets whereas in the column, mass transfer took place by bubbles rising in pool of scrubbing solution.

Some of the assumptions that were made to simplify the solution while modeling the mass transfer in venturi and column are [15]:

- Rate of reaction is assumed to be kinetically fast;;
- Mass transfer is gas film-controlled reaction;
- Gas is considered as incompressible;
- Droplet temperature is assumed to be constant;
- Iodine is transferred from air to water only;
- All liquid droplets and bubbles are assumed to be spherical and no coalescence between them;
- The droplets size and bubble size are represented by a Sauter mean diameter;

Following the above-mentioned assumptions, mass transfer rate of iodine in a droplet of water is given by [15].

$$N_l = 4\pi r_d^2 k_G m(C_{in} - C_i) \tag{1}$$

Mass balance equation for gas enveloping the droplet is

$$N_l = -V\frac{d(mC_{in})}{dt} \tag{2}$$

Sauter Mean diameter of water droplet was calculated by using correlation of Boll et al. because the implemented gas flowrates were within its range [8].

$$d_d = \frac{4.22\times10^{-2} + 5.7\times10^{-3}\left(1000\left(\frac{Q_l}{Q_g}\right)\right)^{1.932}}{v_r^{1.602}} \tag{3}$$

The number of droplets and volume of gas surrounding droplet were calculated by equations provided by Ravindram et al., for venturi scrubber [23].

Number of droplets were calculated by following equation. Liquid film fraction was calculated, and it was insignificant. So, it was assumed that all the injected liquid flowrate got transformed into droplets and number of droplets were calculated by using total liquid flowrate

$$N_d = \frac{Q_l}{V_d} \tag{4}$$

And considering droplets are spherical, we have

$$V_d = \frac{4}{3}\pi r_d^3 \tag{5}$$

Volume of gas surrounding the droplet is given by

$$V = \frac{Q_g}{N_d} \tag{6}$$

The mass transfer coefficient was calculated by using Sherwood number formula

$$Sh = \frac{K_G d_d}{D_g} \tag{7}$$

Sherwood number was calculated using Steinberger and Treybal correlation for the ranges of 1<Re < 30,000 and 0.6<Sc < 30,000 which made it valid for current research [24].

$$Sh = 2 + 0.347\left(ReSc^{0.5}\right)^{0.62} \tag{8}$$

where,

$$\mathrm{Re} = \frac{\rho_g d_d V_g}{\mu_g} \tag{9}$$

$$Sc = \frac{\mu_g}{\rho_g D_g} \tag{10}$$

Contact time of liquid and gas in venturi was calculated by

$$t = \frac{\pi}{4Q_t}\left[(d_{th})^2 l_{op} + \left(d_{diff}\right)^2 l_{diff}\right] \tag{11}$$

Contact time was calculated by dividing the total volume in which contact of liquid and gas took place with total flowrate of liquid and gas. Contact started at the orifice plane in the throat and went on till the end of diffusing section. The total length of throat section was 15 mm, but the orifice plane was present at 12 mm. That means contact took place on total of 3 mm length of throat. So, we used the length from orifice plane's location till the end of throat named as l_{oc} plus the length of diffusing section l_{diff}.

From comparison of (1) and (2) and then integration, we got

$$C_{out} = C_{in}\left[\exp\left(-\frac{4\pi r^2 K_G t}{V}\right)\right] \tag{12}$$

Here, C_i represents the concentration at interface. Theoretical efficiency of venturi was calculated by using

$$E = 1 - \frac{C_{out}}{C_{in}} \tag{13}$$

2.2. Mass transfer model for removal efficiency in column

In the column, similarly, mass transfer from bubbles to liquid is also controlled by gas film.

Mass transfer rate of iodine in a bubble is given by [15].

$$N_l = 4\pi r_b^2 k_G m\left(C'_{in} - C_i\right) \tag{14}$$

Mass balance equation for gas is

$$N_l = -V_b\frac{d\left(mC'_{in}\right)}{dt} \tag{15}$$

Diameter of bubble was calculated by using correlation of Wilkinson et al., applicable to pressure range of 0.1–1.5 MPa [25].

$$d_b^2 = \frac{\sigma}{g\rho_l}\left[8.8\left(\frac{v_g\,\mu_l}{\sigma}\right)^{-0.04}\left(\frac{\sigma^3\rho_l}{g\mu_l^4}\right)^{-0.12}\left(\frac{\rho_l}{\rho_g}\right)^{0.22}\right] \tag{16}$$

Number of bubbles produced were calculated by

$$N_b = \frac{Q_g}{V_b} \tag{17}$$

And considering bubbles as spherical, volume of bubbles was calculated by

$$V_b = \frac{4}{3}\pi r_b^3 \tag{18}$$

Inorganic salt solution mixture of sodium hydroxide and sodium thiosulphate did not let the transformation from homogenous to heterogenous flow to take place. So, size of bubbles was considered to be constant and non-uniform bubble velocity was also not considered. After going up, bubble achieved a constant terminal velocity [26]. Terminal velocity of bubbles was estimated by [27].

$$v_b = \frac{1}{18}\frac{g d_b^2 (\rho_l - \rho_g)}{\mu_l} \tag{19}$$

Mass transfer coefficient was calculated by using Sherwood number formula

$$Sh = \frac{K_G d_b}{D_g} \tag{20}$$

where Sherwood number was calculated by using Steinberger and Treybal correlation [28].

$$Sh = 2 + 0.347\left(ReSc^{0.5}\right)^{0.62} \tag{21}$$

For Reynolds number, following equation was used

$$Re = \frac{\rho_l v_b d_b}{\mu_l} \tag{22}$$

Schmidt number was calculated by (10).

Contact time between gas and liquid in the column is given by

$$t = \frac{\acute{l_l} - l_{venturi}}{v_{br}} \tag{23}$$

Here, contact time was calculated by dividing the length of column in which liquid and gas came in contact with bubble rise velocity. Here $\acute{l_l}$ was length of liquid in the column plus the length added to it due to gas holdup and $l_{venturi}$ was the length of venturi which was subtracted because mass transfer via bubble did not take place there.

where $\acute{l_l}$ was calculated by using the equation $\varepsilon_g = \frac{\acute{l_l} - l_l}{\acute{l_l}}$ here l_l is the length of liquid in the column.

By adding this in equation 25, it became

$$t = \frac{1}{v_{br}}\left[\frac{l_l}{(1-\varepsilon_g)} - l_{venturi}\right] \tag{24}$$

where ε_g was calculated by using Sasaki et al., empirical correlation [13].

$$\varepsilon_g = \frac{C_1 Fr_H}{1 + C_2 Fr_H}$$

$$\text{where } Fr_H = \frac{v_{sg}}{\sqrt{gH_o}},\ C1 = 19.2\ \&\ C2 = 56.4 \tag{25}$$

Interfacial area was calculated by using this formula [29].

$$a = \frac{6\varepsilon_g}{d_b} \tag{26}$$

From comparison of (15) & (16) and then integration led to

$$\acute{C}_{out} = \acute{C}_{in}\left[\exp\left(-\frac{4\pi r_b{}^2 K_G t}{V_b}\right)\right] \tag{27}$$

Here $\acute{C}_{in}$ was the outlet concentration obtained at the exit of venturi.

Removal efficiency of column was calculated by using

$$E = 1 - \frac{\acute{C}_{out}}{\acute{C}_{in}} \tag{28}$$

Overall, total efficiency of venturi scrubber was calculated by

$$E_{tot} = 1 - \frac{\acute{C}_{out}}{C_{in}} \tag{29}$$

3. Experimental setup

Experimental setup for this research can be seen in Fig. 2. In order to simulate the high-pressure scenario in nuclear accidents, the compressed air from a compressor was used. Compressed air enters the pressure regulator followed by a moisture separator and then a rotameter. Air is then heated by a heater to 125°C. For these experiments, temperature is maintained above sublimation temperature of iodine. This high temperature is maintained in order to keep iodine in gaseous form, otherwise iodine deposition inside the line can occur. This heated air is then passed through a well-insulated pipe wrapped with glass wool and heat tracing wire and gets mixed with 1000 ppm (where 1 ppm = 1 mg/kg) iodine solution in ethanol that is being injected by a diaphragm driven dosing pump. Iodine then gets mixed into incoming air and enters the scrubbing column containing a submerged venturi and the scrubbing solution containing 0.2% sodium thiosulphate and 0.5% sodium hydroxide solution. The temperature of the scrubbing column was in the range 40–50°C. Iodine does not desublime in the scrubbing solution because temperature of solution is above saturate value under subsequent partial pressure. Trap bottles have been placed at inlet and outlet with 200 ml (0.1 M KOH) solution. Inlet and outlet samples from the traps are then analyzed by UV-VIS Spectroscopy.

Samples are collected after every 15 min from trap bottles throughout the experiment. 3 outlet traps bottles containing 0.1M KOH solution are placed in series. Leftover iodine from the column gets trapped in these bottles. Iodine reacts with KOH and gets converted into iodide and iodate ions. Further addition of 0.1 M KI and phosphoric acid into these samples leads to formation of triiodide ions. Calibration curve is plotted with known concentrations of iodine in 0.1 KOH solution with added 0.1M KI and phosphoric acid. Unknown concentration is measured against this curve.

Keeping in view the operating parameters described in Table 2, experiments are performed by varying liquid level height from 2.5– 4.5 ft, along with varying air flow rate from 4.5- 6.5 m^3/h. Total run time of experiments is 1 h. Whole setup line is thoroughly washed before and after each experiment. Venturi used in these experiments is made of brass, scrubbing column is made of Perspex and stainless-steel pipes are used in setup. Dimensions of the venturi employed in the experiment can be seen in the Fig. 3. The column height is 6 ft, and its diameter is 0.2 ft.

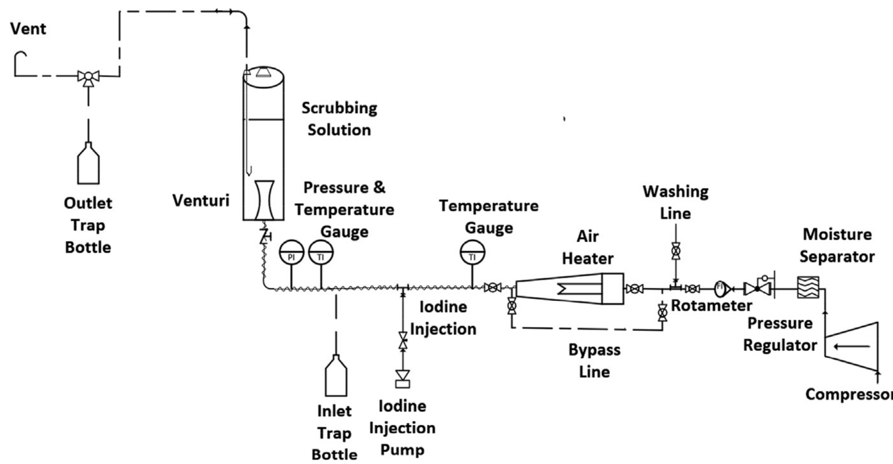

Fig. 2. Schematic diagram of experimental setup.

Table 2
Operating parameters.

Parameter	Value
Maximum Pressure	6 bar
Gas Flowrate	4.5–6.5 m^3/h
Static Head	2.5–4.5 ft.
Iodine Concentration	1000 ppm
Maximum Temperature	125°C

4. Results and discussion

Results of the set of performed experiments are discussed in detail in the following sections.

4.1. Effect of gas flowrate and liquid level height on removal efficiency

Gas flowrate and liquid level height were varied to see their effect on removal efficiency of iodine as given in Fig. 4. Removal efficiency appeared to be increasing with increase in gas flowrate and liquid level height up to a certain optimum point after that it began to decrease. At a gas flowrate of 4.5 m^3/h, liquid level height was varied from 2.5 to 4.5 ft. Initially, as the liquid level was increased, the removal efficiency increased as well. The increase became more drastic with each increment in liquid level height until 4 ft. At 4.5 ft, results started to get saturated. Then at 5 m^3/h gas flowrate, increase in removal efficiency was observed as well as the liquid level height was varied from 2.5 to 4.5 ft. The rise initially became more drastic with each increment in liquid level height but after 4 ft there was no significant increase in removal efficiency. The

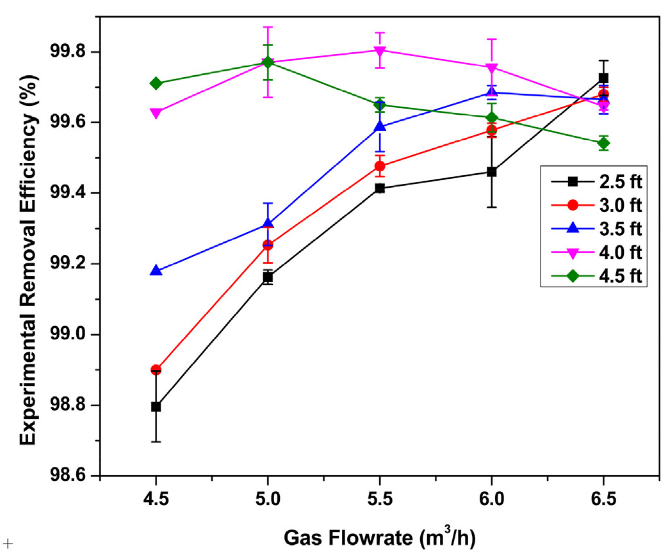

Fig. 4. Effect of gas flowrate and liquid level height on iodine removal efficiency.

increase in removal efficiency at 4 and 4.5 ft liquid level head at 5 m^3/h gas flowrate was even less significant than increase at similar liquid level height at 4.5 m3/h. At 5.5 m^3/h gas flowrate, removal efficiency was observed to be increasing with increase in liquid level height till 4 ft and then a decrease in removal efficiency was observed at 4.5 ft. At 6 m^3/h, the results showed an increase in efficiency till 3.5 ft, a fall in the efficiency was then observed at 4 ft followed by a slightly sharper decline at 4.5 ft. At 6.5 m^3/h, increase in removal efficiency was observed only at 2.5 ft after that,

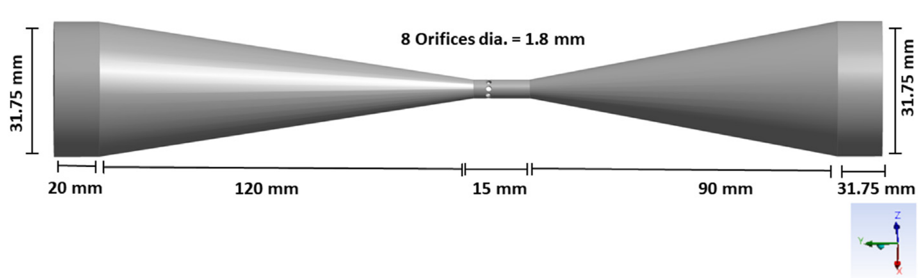

Fig. 3. Dimensions of venturi.

efficiency slightly decreased with each increment in liquid level height and the fall got prominent at 4 ft. Maximum removal efficiency of 99.8% was achieved at 5.5 m^3/h and 4 ft liquid level height.

Increase in gas flowrate and liquid level height both caused an increase in pressure drop. This increase in pressure drop led to an increase in removal efficiency. Increase in gas flowrate increased the throat velocity which enhanced the rate of impaction between droplet and gas phase at throat. It also produced finer and larger number of droplets thereby increasing the removal efficiency. At low gas flowrates, increase in liquid head caused an increase in driving pressure difference between the outer and inner region of the throat hence, causing more suction of liquid and increasing the induced flow of liquid. Due to this, more liquid got injected via orifices, more contact of liquid with gas took place and a larger number of droplets were produced. At high gas flowrates, beyond an optimum limit, increase in gas velocity caused the droplets to achieve throat velocity very quickly giving it very less time to interact with liquid and hence removal efficiency started to decrease beyond that point. Although finer droplets were produced, the volume of gas surrounding the liquid got increased as well due to which less contact of gas and liquid took place and as a result decrease in removal efficiency was observed. At high flowrates, turbulence and non-uniform flux distribution also caused reduction in removal efficiency.

At high gas flowrates, increase in liquid level height beyond the optimum value caused excessive jet penetration, causing the jet to be atomized close to the wall aiding the deposition of droplets. This resulted in decrease of liquid available for contact with gas in the form of droplets and hence, causing decrease in the removal efficiency with increase in liquid head beyond that point.

4.2. Relationship between induced liquid flow and gas flowrates

Fig. 5. illustrates that variation in induced liquid flow into throat caused by variation in gas flowrate. Liquid flowrate was measured experimentally. For liquid flowrate measurement, venturi scrubber was placed outside the scrubbing column at a specific height and water got injected automatically into the venturi scrubber due to pressure difference. The decrease in level of water was measured along with the time. The flowrate of liquid was calculated by using following formula.

$$Q_l = \frac{V_l}{t} \tag{30}$$

Where Q_l is flowrate of liquid, V_l is the volume of water reservoir and t is the elapsed time. At a constant liquid level height, the induced liquid flow appeared to be decreasing with increase in gas flowrate. The liquid got injected due to pressure difference between outside and inside the throat. Increase in gas flowrate caused the static pressure to increase. The increase in pressure caused the pressure difference between outside and inside the throat to decrease and as a result decreased the liquid flow. At a constant gas flowrate, liquid flow was increased with increasing liquid level height because of increase in hydrostatic pressure. This caused the pressure gradient to increase, and more water was injected, as a result, into the throat, hence increasing the liquid flow.

4.3. Effect of gas flowrate on inlet iodine concentration

Effect of gas flowrate on inlet iodine concentration has been shown in Fig. 6. Decrease in iodine concentration with increase in gas flowrate was observed when mass flowrate of iodine was kept fixed.

4.4. Gas holdup

Variation of gas holdup with gas flowrate and liquid head is shown in Fig. 7. Results showed an increase in gas holdup with increasing the gas flowrate. The superficial velocity was increased with increase in the gas flowrate and this increase caused a decrease in the diameter and increase in number of bubbles. The smaller the bubbles, the smaller the rise velocity, which increased the contact time between gas and liquid thus increasing the gas holdup. Increase in liquid level height caused the bubbles to become larger in size and their rise velocity increased as well, thereby giving less time for liquid and gas to contact and decreasing the gas hold up [9–11,14,30]. Experimental calculation of gas holdup was done by using the following formula

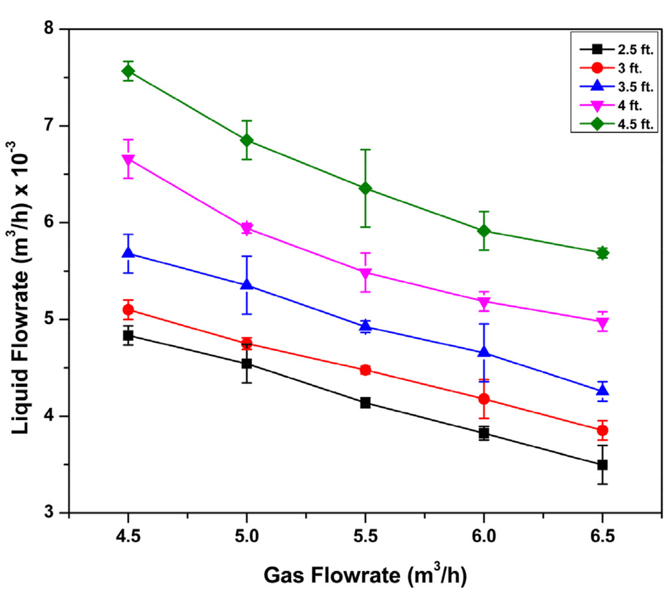

Fig. 5. Effect of gas flowrate on induced liquid flowrate.

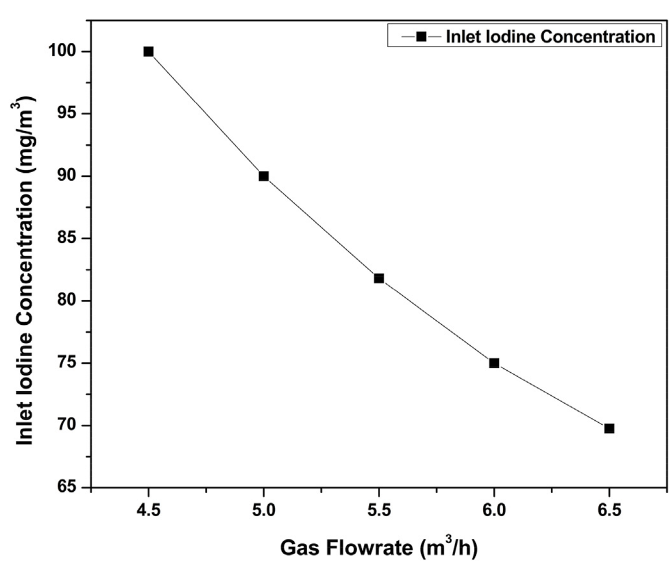

Fig. 6. Effect of gas flowrate on inlet iodine concentration.

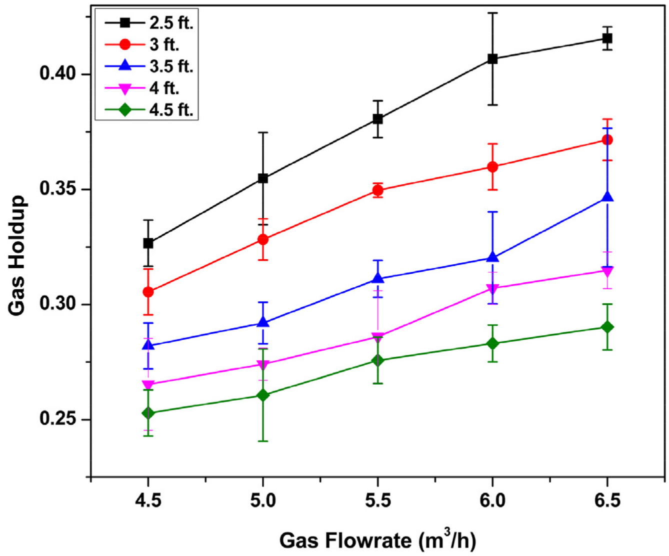

Fig. 7. Effect of gas flowrate and liquid level height on gas holdup.

$$\varepsilon_g = \frac{V_{gh} - V_l}{V_{gh}} \tag{31}$$

4.5. Comparison of gas holdup

Experimental data of gas hold up was compared with different correlations. The results showed good agreement with sasaki et al., correlation [13]as shown in Fig. 10. Hughmark [9], Hikita et al. [14], Hikita and Kikukawa [10], Kumar et al. [11],and sal et al. [12],all studied the effect of superficial gas velocity on gas holdup but did not consider effect of liquid height. The liquid height and superficial gas velocity were both incorporated in the correlation by sasaki et al.,. As observed in Fig. 8, gas hold up depended on both liquid height and superficial gas velocity. That is why the experimental results showed good good agreement with the sasaki et al., results [13].

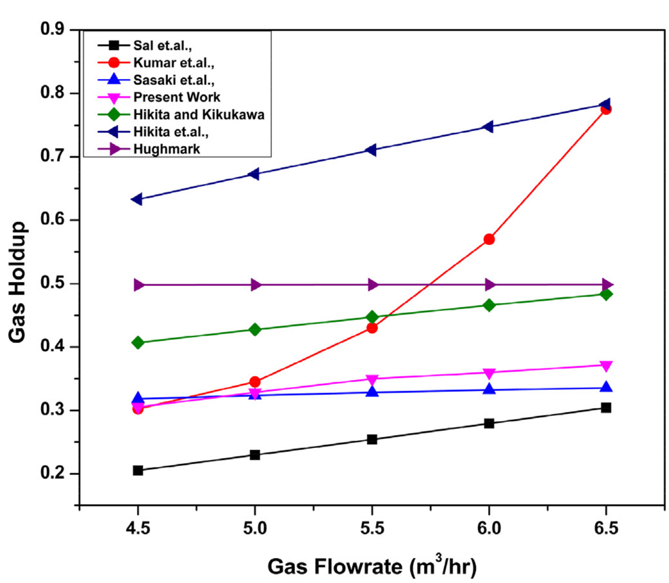

Fig. 8. Comparison of experimental and predicted gas holdup.

4.6. Interfacial area

Variation of interfacial area with variation of gas flowrate and liquid head is shown in Fig. 9. Increase in gas flowrate produced small and larger number of bubbles with small rise velocity. So, this increased the interfacial area of contact for liquid and gas. The increase in liquid head produced bubbles of large size but small in number. The large bubbles quickly got accelerated due to high rise velocities thereby decreasing the interfacial area of contact for liquid and gas [29,31,32].

4.7. Comparison of theoretical and experimental results of removal efficiency

The predicted results of removal efficiency from the model were compared with the experimental results. The results were observed to be in good agreement. Overall ± 5 % Error was calculated. It can be seen in Fig. 10 and Fig. 11. Overall, results of model agree well with experimental results with a maximum error of 5 %. At high flowrates, decrease in removal efficiency was observed in experimental results. Many factors have contributed to this apparent decrease in experimental results. When the gas and liquid flowrates are increased beyond an optimum point, factors like non-uniform flux distribution, decrease in contact of gas and liquid due to very high velocity of gas and turbulence caused by interaction among droplets cause reduction in the removal efficiency. Absence of these factors in the model can be the possible cause of deviation in the predicted results. Incorporation of non-uniform flux distribution and interaction among droplets along the length of venturi in the model is very cumbersome and will likely enhance the complexity of model. Not to mention that error in Fig. 11 d) and e) are very small.

5. Conclusion

Following conclusions were obtained from the results.

Venturi Scrubber must be operated at optimum values of gas flowrate and liquid head to get maximum removal efficiency. Therefore, optimum values of liquid and gas flowrates were determined and beyond the optimum values, the efficiency decreased due to bad coverage at throat and less contact of liquid

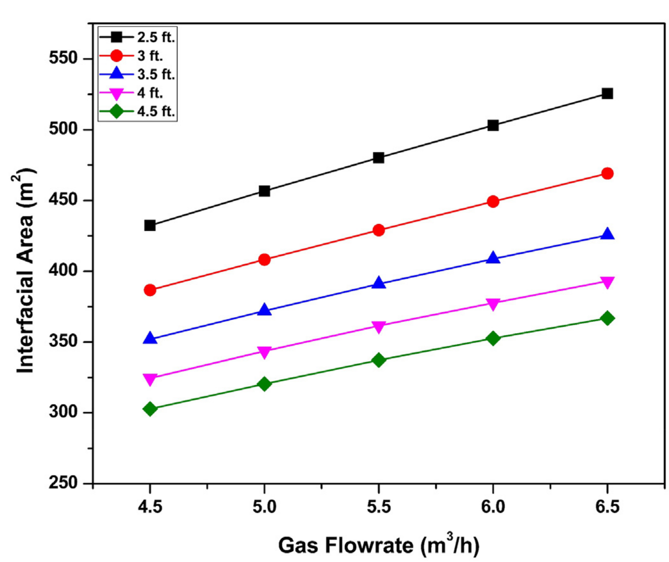

Fig. 9. Effect of gas flowrate and liquid head on interfacial area.

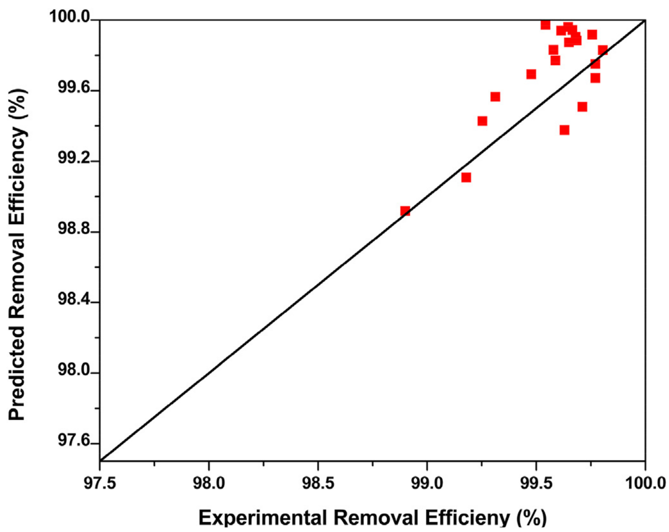

Fig. 10. Comparison of experimental and predicted removal efficiency.

and gas. The effect of other parameters was observed as well. Jet penetration length increased with increase in gas flowrate and decreased with increase in liquid flowrate. Decrease in bubble diameter was observed with increase in the gas flowrate causing more no. of bubbles to be formed. These small bubbles had low rise velocity so, the interfacial area of contact and residence time increased causing gas hold up to increase. When the liquid level height was increased, the bubble diameter increased as well, and a smaller number of bubbles were produced. These large size bubbles had high rise velocity so, they accelerated quickly causing residence time, interfacial area of contact and gas holdup to be decreased. Gas hold up was compared with 6 correlations and experimental results were in good agreement with Sasaki et al. [1], results because liquid height was considered in this correlation. Gas holdup was observed to increase with increase in superficial gas velocity and decrease with increase in liquid height. The addition of penetration length, bubble rise velocity and gas holdup in contact improved the mathematical model and the predicted results were in good agreement with experiment results. Maximum removal efficiency of 99.8% was achieved which agreed well with the requirement for filtered containment venting system.

Declaration of competing interest

The authors declare that they have no known competing financial interests or personal relationships that could have appeared to influence the work reported in this paper.

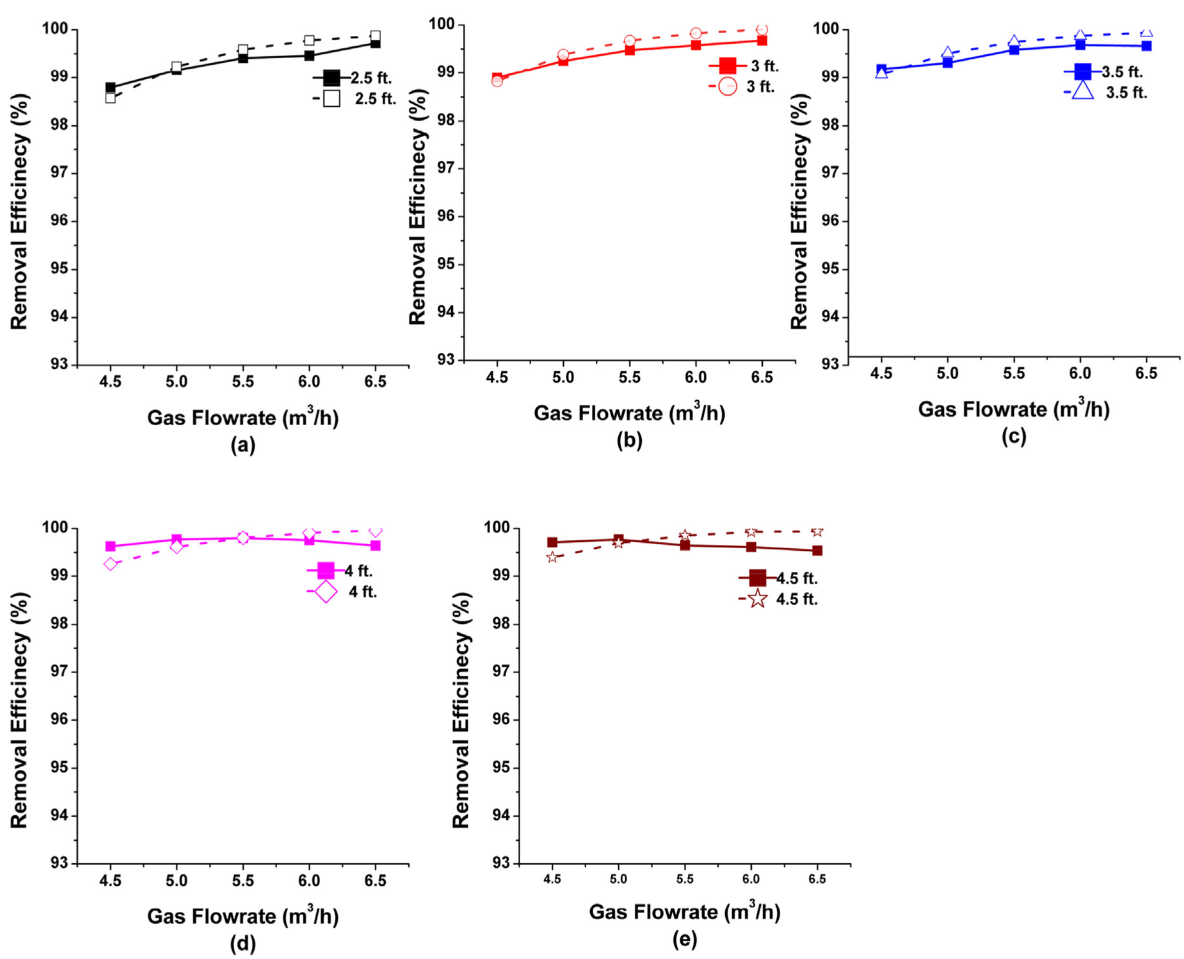

Fig. 11. Comparison of Removal Efficiency at a) 2.5 ft. Liquid Head (b) 3 ft. Liquid Head (c) 3.5 ft. Liquid Head (d) 4 ft. Liquid Head (e) 4.5 ft. Liquid Head (Solid Symbol: Experimental Results; Hollow Symbols: Predicted Results).

Nomenclature and Abbreviations

A	Interfacial Area / m^{-1}
C_i	Concentration at interface / ppm
C_{in}	Concentration of Iodine at the Entrance of Converging Section of Venturi / ppm
C_{in}'	Concentration of Iodine at the Exit of Diverging Section of Venturi / ppm
C_{out}	Concentration of Iodine at the Exit of Diverging Section of Venturi / ppm
C_{out}'	Concentration of Iodine at the Exit of Column / ppm
d_b	Bubble Diameter / m
d_c	Diameter of Column / m
d_d	Droplet Diameter / m
D_g	Gas Diffusion Co-efficient / m^2s^{-1}
d_o	Orifice Diameter / m
d_{th}	Diameter of Throat / m
E	Removal Efficiency at the End of Venturi / %
E_o	Eotvos Number
E'	Overall Removal Efficiency at the End of Column / %
Fr	Froude Number
Fr_H	Froude Number Using Liquid Height
g	Gravitational Acceleration / m/ s^2
k_g	Gas Mass Transfer Co-efficient / m^{-1}
l_{con}	Length of Converging Section / m
l_{diff}	Length of Diverging Section / m
l_l	Length of Liquid in the Column / m
l_l'	Length of Liquid Plus Added Height due to Gas Holdup in the Column / m
l_{op}	Length from Orifice Plane to the End of Throat Section / m
l_{vent}	Length of Venturi / m
l*	Penetration Length / m
m	Distribution Parameter /
N_b	Number of Droplets Produced per Second / sec
N_d	Number of Bubbles Produced per Second / sec
N_l	Mass Transfer in a Single Droplet /
n_o	Number of Orifices
Q_g	Volumetric Flowrate of Gas / m^3/s
Q_l	Volumetric Flowrate of Liquid / m^3/s
Q_t	Total Flowrate of Liquid and Gas
r_b	Radius of Bubble / m
r_d	Radius of Droplet / m
Re	Reynolds Number
r_{th}	Radius of Throat / m
Sc	Schmidt Number
Sh	Sherwood Number
t	Contact Time between Liquid and Gas / s
v_g	Velocity of Gas / m/s
v_l	Velocity of Liquid / m/s
v_{br}	Bubble Rise Velocity / m/s
v_r	Relative Velocity / m/s
v_{sg}	Superficial Gas Velocity / m/s
V	Volume of Gas Surrounding Droplet / m^3
V_{gh}	Volume of Liquid Plus Gas Holdup in the Column / m^3
V_b	Volume of Bubble / m^3
V_l	Volume of Liquid in Column / m^3
W_{th}	Width of Throat / m
We	Weber Number

Greek Letters

ε_g	Gas Holdup
ρ_g	Gas Density / kg/m3
ρ_l	Liquid Density / kg/m3
μ_g	Gas Viscosity / kg/ms
μ_l	Liquid Viscosity / kg/ms
σ_l	Surface Tension of Liquid / N/m

References

[1] K. Shozugawa, N. Nogawa, M. Matsuo, Deposition of fission and activation products after the Fukushima Dai-ichi nuclear power plant accident, Environmental Pollution 163 (2012) 243–247, https://doi.org/10.1016/j.envpol.2012.01.001.

[2] T.J. Solaija, N. Irfan, K.R. Qureshi, K. Waheed, A. Farooq, M. Ahmad, Filtered Containment Venting System (FCVS) for removal of elemental and organic iodine during severe nuclear power plant accidents, in: 2017 3rd International Conference on Power Generation Systems and Renewable Energy Technologies (PGSRET), IEEE, 2017, pp. 61–66, https://doi.org/10.1109/PGSRET.2017.8251802.

[3] IAEA, Severe Accident Mitigation through Improvements in Filtered Containment Vent Systems and Containment Cooling Strategies for Water Cooled Reactors, 2017. IAEA-TECDOC-1812.

[4] B. Handley, C. Coon, D.M. Marshall, Principles of Engineering, Cengage Learning, 2012.

[5] H.F. Johnstone, R.B. Feild, M.C. Tassler, Gas absorption and aerosol collection in a venturi atomizer, Industrial & Engineering Chemistry 46 (1954) 1601–1608, https://doi.org/10.1021/ie50536a028.

[6] S. Ali, K. Waheed, K. Qureshi, N. Irfan, M. Ahmed, W. Siddique, A. Farooq, Experimental Investigation of Aerosols Removal Efficiency through Self-Priming Venturi Scrubber, Nuclear Engineering and Technology, 2020, https://doi.org/10.1016/j.net.2020.03.019.

[7] S. Nukiyama, An experiment on the atomization of liquid by means of an air stream (1), J. Soc. Mech. Eng., Japan. 4 (1938) 128–135, https://doi.org/10.1299/kikai1938.4.15_138.

[8] R.H. Boll, L.R. Fiais, P.W. Maurer, W.L. Thompson, Mean drop size in a full scale venturi scrubber via transmissometer, Journal of the Air Pollution Control Association 24 (1974) 934–938, https://doi.org/10.1080/00022470.1974.10469991.

[9] G.A. Hughmark, Holdup and mass transfer in bubble columns, Industrial & Engineering Chemistry Process Design and Development 6 (1967) 218–220, https://doi.org/10.1021/i260022a011.

[10] H. Hikita, H. Kikukawa, Gas holdup in bubble columns. Effect of liquid properties, Bull. Univ. Osaka Prefect. Ser. A. 22 (1973) 151–160, https://doi.org/10.1021/i260045a015.

[11] S. Kumar, R.A. Kumar, P. Munshi, A. Khanna, Gas hold-up in three phase co-current bubble columns, Procedia Engineering 42 (2012) 782–794, https://doi.org/10.1016/j.proeng.2012.07.470.

[12] S. Şal, Ö.F. Gül, M. Özdemir, The effect of sparger geometry on gas holdup and regime transition points in a bubble column equipped with perforated plate spargers, Chemical Engineering and Processing: Process Intensification 70 (2013) 259–266, https://doi.org/10.1016/j.cep.2013.03.012.

[13] S. Sasaki, K. Hayashi, A. Tomiyama, Effects of liquid height on gas holdup in air–water bubble column, Experimental Thermal and Fluid Science 72 (2016) 67–74, https://doi.org/10.1016/j.expthermflusci.2015.10.027.

[14] H. Hikita, S. Asai, K. Tanigawa, K. Segawa, M. Kitao, Gas hold-up in bubble columns, The Chemical Engineering Journal 20 (1980) 59–67, https://doi.org/10.1016/0300-9467(80)85006-4.

[15] B.J. Azzopardi, S. Teixeira, A.H. Govan, T.R. Bott, Improved model for pressure drop in venturi scrubbers, Process Safety and Environmental Protection 69 (1991) 237–245.

[16] X. Gamisans, M. Sarra, F.J. Lafuente, The role of the liquid film on the mass transfer in venturi-based scrubbers, Chemical Engineering Research and Design 82 (2004) 372–380, https://doi.org/10.1205/026387604322870480.

[17] M. Ali, C. Yan, Z. Sun, H. Gu, J. Wang, Study of iodine removal efficiency in self-priming venturi scrubber, Annals of Nuclear Energy 57 (2013) 263–268, https://doi.org/10.1016/j.anucene.2013.02.014.

[18] M. Ali, Y. Changqi, S. Zhongning, G. Haifeng, W. Junlong, K. Mehboob, Iodine removal efficiency in non-submerged and submerged self-priming venturi scrubber, Nuclear Engineering and Technology 45 (2013) 203–210, https://doi.org/10.5516/NET.03.2012.047.

[19] N.P. Gulhane, A.D. Landge, D.S. Shukla, S.S. Kale, Experimental study of iodine removal efficiency in self-priming venturi scrubber, Annals of Nuclear Energy 78 (2015) 152–159, https://doi.org/10.1016/j.anucene.2014.12.008.

[20] M. Bal, T.T. Reddy, B.C. Meikap, Performance evaluation of venturi scrubber for the removal of iodine in filtered containment venting system, Chemical Engineering Research and Design 138 (2018) 158–167, https://doi.org/10.1016/j.cherd.2018.08.019.

[21] J. Jung, J.B. Lee, H.Y. Kim, Experimental investigation of iodine decontamination performance of a filtered containment venting system in ARIEL facility, in: Proceeding of the 26th International Conference Nuclear Energy for New Europe, Bled, Slovenia, 2017.

[22] Y. Zhou, Z. Sun, H. Gu, Z. Miao, Performance of iodide vapour absorption in the venturi scrubber working in self-priming mode, Annals of Nuclear Energy 87 (2016) 426–434, https://doi.org/10.1016/j.anucene.2015.09.026.

[23] M. Ali, C. Yan, Z. Sun, H.F. Gu, M. Wang, Study of pressure drop model for self-priming venturi scrubber, in: 2012 Asia-Pacific Power and Energy Engineering

Conference, IEEE, 2012, pp. 1–4, https://doi.org/10.1109/APPEEC.2012.6306987.
[24] M. Ravindram, P. Naidu, Modeling of a venturi scrubber for the control of gaseous pollutants, Industrial Engineering Chemistry Process Design Development 25 (1986) 35–40, https://doi.org/10.1021/ie00066a037.
[25] P.M. Wilkinson, H. Haringa, L.L. van Dierendonck, Mass transfer and bubble size in a bubble column under pressure, Chemical Engineering Science 49 (1994) 1417–1427, https://doi.org/10.1016/0009-2509(93)E0022-5.
[26] J. Wen, H. Gu, Z. Sun, Y. Zhou, A theoretical model and experiment validation on filtration characteristics of methyl iodide in bubble column, International Journal of Heat Mass Transfer 114 (2017) 1263–1273, https://doi.org/10.1016/j.ijheatmasstransfer.2017.07.023.
[27] M.A.R. Talaia, Terminal velocity of a bubble rise in a liquid column, World Academy of Science, Engineering Technology 28 (2007) 264–268.
[28] R.L. Steinberger, R.E. Treybal, Mass transfer from a solid soluble sphere to a flowing liquid stream, AIChE Journal 6 (1960) 227–232, https://doi.org/10.1002/aic.690060213.
[29] K. Akita, F. Yoshida, Bubble size, interfacial area, and liquid-phase mass transfer coefficient in bubble columns, Industrial & Engineering Chemistry Process Design and Development 13 (1974) 84–91, https://doi.org/10.1021/i260049a016.
[30] A. Mandal, G. Kundu, D. Mukherjee, A comparative study of gas holdup, bubble size distribution and interfacial area in a downflow bubble column, Chemical Engineering Research and Design 83 (2005) 423–428, https://doi.org/10.1205/cherd.04065.
[31] M. Bouaifi, G. Hebrard, D. Bastoul, M. Roustan, A comparative study of gas hold-up, bubble size, interfacial area and mass transfer coefficients in stirred gas–liquid reactors and bubble columns, Chemical Engineering and Processing: Process Intensification 40 (2001) 97–111, https://doi.org/10.1016/S0255-2701(00)00129-X.
[32] R. Maceiras, E. Álvarez, M.A. Cancela, Experimental interfacial area measurements in a bubble column, Chemical Engineering Journal 163 (2010) 331–336, https://doi.org/10.1016/j.cej.2010.08.011.